Carbohydrate Polymers 117 (2015) 722–730

Contents lists available at ScienceDirect

Carbohydrate Polymers

journal homepage: www.elsevier.com/locate/carbpol

Incorporation of chitosan in biomimetic gelatin/chondroitin-6-sulfate/hyaluronan cryogel for cartilage tissue engineering

Chang-Yi Kuo [a,1], Chih-Hao Chen [a,b,1], Chien-Yu Hsiao [c], Jyh-Ping Chen [a,c,*]

[a] Department of Chemical and Materials Engineering, Chang Gung University, Kwei-San, Taoyuan 333, Taiwan, ROC
[b] Craniofacial Research Center, Department of Plastic and Reconstructive Surgery, Chang Gung Memorial Hospital, Chang Gung University, College of Medicine, Kwei-San, Taoyuan 333, Taiwan, ROC
[c] Research Center for Industry of Human Ecology, Chang Gung University of Science and Technology, Kwei-San, Tao-Yuan 333, Taiwan, ROC

ARTICLE INFO

Article history:
Received 27 May 2014
Received in revised form 7 October 2014
Accepted 21 October 2014
Available online 30 October 2014

Keywords:
Chitosan
Chondroitin sulfate
Hyaluronan
Cryogel
Cartilage tissue engineering
Gelatin

ABSTRACT

We prepare an elastic macroporous gelatin/chondoitin-6-sulfate/hyaluronan (GCH) cryogel scaffold mimic the composition of cartilage extracellular matrix for cartilage tissue engineering. By incorporating chitosan in the cryogel to replace 20% gelatin, a GCH-chitosan cryogel was also synthesized and compared with GCH cryogel for scaffold mechanical properties and chondrocytes response. The GCH-chitosan cryogel has larger pores, higher ultimate strain (stress) and elastic modulus, and lower stress relaxation percentage than the GCH cryogel. Both cryogels show a highly elastic property with a loss tangent around 0.1, but chitosan incorporation increases the storage modulus (elasticity). Chondrocytes proliferate and redifferentiate in cryogels; chitosan diminishes cell proliferation but up-regulates glycosaminoglycans (GAGs) and type II collagen (COL II) secretion. Implantation of a chondrocytes/GCH-chitosan cryogel construct in a full-thickness articular cartilage defect regenerates cartilage with positive stainings for GAGs and COL II and an elastic modulus similar to the native cartilage.

1. Introduction

Functional tissue constructs for cartilage defects can be prepared by isolating viable chondrocytes from the patient, expanding the cell population, culturing cells in vitro on a scaffold, and then implanting the resulted tissue engineered construct back into the patient (Vacanti, 2003). In this approach, the biodegradable three-dimensional scaffold acts like an artificial extracellular matrix (ECM) while temporarily serves as a template to guide cell adhesion, proliferation and tissue development. For tissue engineering purpose, the scaffold should have an interconnected open macroporous network to allow unobstructed cell penetration and transport of nutrients, oxygen and waste products. In addition to these essential properties, for engineering soft tissues like cartilage that exhibits elastic properties, elasticity of scaffolds is being looked upon as an important design parameter (Yang, Webb, Pickerill, Hageman, & Ameer, 2006). A scaffold that can maintain its mechanical integrity during cyclic mechanical strains without permanent deformation may be another important criterion.

Cryogels are gel matrices that are synthesized at subzero temperatures using monomeric or polymeric precursors (Lozinsky et al., 2003). These gels can be obtained through the formation of both physically and covalently crosslinked homogeneous or heterogeneous polymer networks. At subzero temperature, most of the solvent gets frozen while part of the solvent is left unfrozen in the liquid microphase where dissolved substances concentrate and undergo chemical reactions (Lozinsky, Plieva, Galaev, & Mattiasson, 2001). These chemical reactions in the liquid microphase lead to gel formation with the crystals of frozen solvent acting as porogens. After thawing the ice crystals, a system of large interconnected pores is formed within the cryogel. Cryogels have some important characteristics including interconnected macroporous structure, mechanical stability and elasticity (Lozinsky et al., 2003). Elastic poly(vinyl alcohol) cryogel has been suggested for cartilage repair in arthritic shoulder replacement (Swieszkowski, Ku, Bersee, & Kurzydlowski, 2006).

Chondroitin-6-sulfate is a sulfated glycosaminoglycan (GAG), composed of a chain of alternating units of glucuronic acid and N-acetylgalactosamine, the latter being sulfated at O6. It is usually

* Corresponding author at: Department of Chemical and Materials Engineering, Chang Gung University, Kwei-San, Taoyuan 333, Taiwan, ROC. Tel.: +886 3 2118800; fax: +886 3 2118668.
E-mail address: jpchen@mail.cgu.edu.tw (J.-P. Chen).
[1] These authors contributed equally to this work.

http://dx.doi.org/10.1016/j.carbpol.2014.10.056
0144-8617/

found attached to proteins as part of a proteoglycan. It is an important structural component of cartilage and provides much of its resistance to compression. Inclusion of chondroitin sulfate in scaffold may promote the secretion of proteoglycan and type II collagen (Sechriest et al., 2000). Hyaluronan (hyaluronic acid) is an anionic, nonsulfated GAG distributed widely distributed throughout connective, epithelial, and neural tissues. As one of the chief components of the ECM, hyaluronan contributes to cell proliferation and migration, and facilitate the integration of engineered cartilage during embryonic cartilage development (Solchaga, Goldberg, & Caplan, 2001). Gelatin is considered as denatured collagen, the major protein component of cartilage, but with relatively low antigenicity and cost than collagen. Crosslinked gelatin and hyaluronan/gelatin scaffolds were shown to be suitable for application in cartilage tissue engineering (Angele et al., 2009; Lien, Li, & Huang, 2008). Chitosan is the cationic (1-4)-2-amino-2-deoxy-β-D-glucan with typical degree of acetylation close to 0.20. Chitosan has recently attracted interests as a candidate for cartilage repair because of its biocompatibility and structural similarity with the GAG present in the ECM of cartilage (VandeVord et al., 2002). Incorporating chitosan in cartilage tissue engineering scaffolds could provide a friendly environment for chondrocytes to propagate, produce typical ECM and maintain the correct phenotype (Muzzarelli, Greco, Busilacchi, Sollazzo, & Gigante, 2012). Chitosan-based porous scaffold was demonstrated to sustain chondrogenesis (Nettles, Elder, & Gilbert, 2002).

The objective of this study is to fabricate a macroporous, elastic cryogel scaffold from gelatin, chondoitin-6-sulfate and hyaluronan, whose chemical environment mimicking that of cartilage ECM (Chang, Liu, Lin, Chou, & Lin, 2003). Since chitosan has the potential to fulfill many of the requirements of a cartilage tissue engineering scaffold material, we further incorporate this GAG analog in the cryogel and study its effect on matrix properties, cell proliferation and differentiation.

2. Materials and methods

2.1. Materials

Sodium hyaluronan (HA, average molecular weight = 1.3 MDa) was obtained from Bloomage Freda Biopharm Co. Ltd. Gelatin (GEL, type A from porcine skin, 300 bloom, average molecular weight = 60 kDa) and chondroitin-6-sulfate (C6S, sodium salt from shark cartilage), chitosan (from shrimp shells, average molecular weight = 150 kDa, degree of deacetylation = 85%) were obtained from Sigma–Aldrich. 1-Ethyl-3-(3-dimethylaminopropyl) carbodiimide (EDC) was obtained from Acros. 2-(N-morpholino)ethanesulfonic acid (MES), 2,4,6-trinitrobenzene sulfonic acid (TNBS), antibiotics and trypsin-EDTA were all purchased from Sigma-Aldrich. Dulbecco's Modified Eagle's Medium/Nutrient Mixture F-12 (DMEM/F-12, Sigma) and fetal bovine serum (FBS, HyClone) were used for cell culture. The 4′,6-diamidino-2-phenylindole (DAPI) solution for cell staining was obtained from Life Technologies.

2.2. Preparation of GCH and GCH-C cryogels

Cryogels were prepared by a modified method reported previously (Chang, Liao, & Chen, 2013). For GCH cryogel, 10% (w/w) GEL and 2% (w/v) C6S/0.1% (w/v) HA solutions were prepared separately at 70 °C and 37 °C in 0.5 M MES buffer (pH 6.0). EDC was added to the C6S/HA solution to a final concentration of 4% (w/v) and mixed for 30 min to obtain the C6S/HA/EDC solution. Two milliliter each of GEL and C6S/HA/EDC solution was added to a 5 ml disposable syringe (13 mm internal diameter), shaken at 70 °C for 30 s and placed in −16 °C ethanol in a deep freezer for 16 h in to complete the crosslinking reaction. After thawing at room temperature, the formed cryogel was pushed out from the syringe and washed by incubating in 1000 ml of phosphate buffered saline (PBS) for 2 h to remove residual EDC and reaction byproducts. Disks (2 mm in thickness and 10 mm in diameter) were cut from the cryogel with a sharp blade and a biopsy puncher and washed again by incubating in 500 ml of 70 °C 0.1 M MES buffer for 4 h to remove non-reacting substances. A final wash by incubating in 1000 ml de-ionized distilled (DDI) water for 12 h removed MES buffer from the cryogel. The preparation of GCH-chitosan cryogel followed the same procedure as GCH cryogel by replacing the 10% (w/w) GEL solution with an 8% (w/w) GEL/2% (w/v) chitosan solution. The final weight percentage of each component is 82.6% GEL, 16.5% C6S and 0.83% HA in the GCH cryogel; 66.1% GEL, 16.5% chitosan, 16.5% C6S and 0.83% HA in the GCH-chitosan cryogel.

2.3. Characteristics of cryogels

Pore size measurement was carried out with capillary flow porometry (PMI CFP-1100-AI, Porous Materials Inc., USA) using ethanol as the wetting agent. Porosity was determined using the ethanol displacement method (Zhang and Ma, 1999). The density of scaffold was calculated by the mass of the dry or wet scaffold over its volume. The microstructure of scaffold was observed by scanning electron microscope (SEM) (Philips XL-30) after sputter coating for 60 s.

Compression behavior of cryogel scaffolds were investigated by unconfined compression tests using an ElectroForce 5200 BioDynamic Test Instrument (Bose) in PBS at 37 °C. Wet samples were used for the tests after soaking in PBS for 24 h prior to testing. The compression load was applied with a 250 N load cell at a crosshead speed of 0.02 mm/s. A stress (σ)–strain (ε) curve was recorded with an uniaxial stress. The point where failure of the cryogel occurred gave the ultimate stress and ultimate strain values. The stress–strain data up to failure were fitted by a non-linear equation (Woo, Gomez, & Akeson, 1981),

$$\sigma = Ae^{(B\varepsilon - 1)} \quad (1)$$

A and B are elastic constants. Elastic modulus at 10% and 30% strain was calculated from this non-linear elastic model from the slope of the tangent to the stress–strain curve. Toughness (compressive strain energy to failure) of a cryogel, defined as the energy necessary to deform a specimen to failure, was obtained from the area under the stress–strain curve.

For evaluating the stress-relaxation behavior, the samples were compressed to 30% strain in 1 s followed by 500 s relaxation to reach steady state. The stress relaxation curve was plotted as remaining stress percentage and curve-fitted according to the non-linear equation (Wan, Campbell, Zhang, Hui, & Boughner, 2002),

$$\sigma_t/\sigma_o = \sigma_R + \alpha e^{-k_1 t} + \beta e^{-k_2 t} \quad (2)$$

σ_t is the stress at time t, σ_o is the initial stress, σ_R is the relative remaining stress at t = 500 s, α and β are proportional constants, k_1 and k_2 are relaxation-rate fitting parameters for the initial and final regions, respectively.

The cyclic compression test was similarly performed by loading the sample to 30% strain with 3200 cycles at a frequency of 1 Hz. The energy absorption in cryogel was derived from the stress–strain relation. A hysteresis loop, bounded by the loading and unloading curves, could be found, indicating dissipation of energy or energy absorbed due to the viscous properties of the cryogel. The dissipation energy (kJ/m^3) loss during the hysteresis cycle was calculated from the area bounded within the hysteresis loop. The percentage of energy dissipation (%) was calculated by dividing the dissipative energy with the area bounded between the loading curve and

the horizontal axis (compression energy), which indicates the total energy applied to the sample during compression.

For dynamic compression testing, the sample was dynamically tested with sinusoidal compressions from 0.5 to 10 Hz at 30% compression. The complex modulus (E^*) is the ratio of the stress to the strain, which can be divided into the energy stored per cycle, or storage modulus (E'), and the energy lost per cycle, or loss modulus (E''). The loss tangent is calculated as $\tan\delta = E''/E'$. For each testing frequency, the dynamic mechanical analysis software measured the values of E^*, E', E'' and $\tan\delta$.

2.4. In vitro cell culture

Chondrocytes were harvested from the knee articular cartilage of rabbits as described previously (Chen and Cheng, 2006). Animal experiments were performed with approval from the Institutional Animal Care and Use Committee of Chang Gung University. After subcultures for three passages, the cells were trypsinized and mixed with DMEM/F12. The cryogel scaffold was placed in a well of a 48-well cell culture plate and sterilized by immersing in 1 ml 75% ethanol for 24 h and overnight exposure to UV light in a sterile tissue culture hood. The scaffold was rinsed three times with 1 ml PBS and immersed in 1 ml DMEM/F12 for 30 min. The excess medium on the scaffold surface was removed and the scaffold was transferred to a new well in a 48-well cell culture plate for cell seeding. An aliquot of 10 μl of a cell suspension (1×10^7 cells/ml) was seeded directly onto the surface of the wet cryogel disk in each well. Cell-seeded cryogels were incubated at 37 °C for 2 h to allow cell attachment and 2 ml of DMEM/F12 containing 10% FBS and 1.0% streptomycin–penicillin solution was added to each well. The constructs were cultured at 37 °C in humidified 5% CO_2 for 21 d with medium change every 3 d. The construct were harvested at predetermined times and digested in 1 ml papain solution (55 mM sodium citrate, 150 mM sodium chloride, 5 mM cysteine HCl, 5 mM EDTA and 0.2 mg/ml papain) at 60 °C for 24 h to determine the DNA content. The total sulfated glycosaminoglycan (sGAG) and collagen type II (COL II) contents were determined at the same time points by considering both the intracellular amount in the construct and the extracellular amount in the culture medium. The DNA content was determined using Hoechst 33258 (Kim, Sah, Doong, & Grodzinsky, 1988), and the sGAG content was determined using 1,9-dimethylmethylene blue with C6S as the standard (Enobakhare, Bader, & Lee, 1996). The COL II content was determined quantitatively using sandwich ELISA with rabbit anti-COL II polyclonal antibody (Biorbyt orb10436) and HRP conjugated rabbit anti-COL II polyclonal antibody (Bioss bs-0709R-HRP). For SEM analysis, the chondrocyte/cryogel constructs cultured for 21 d were fixed with 2.5% glutaraldehyde for 24 h at room temperature. After thorough washing with 0.1 M PBS (pH 7.4), the samples were dehydrated in ethanol in a sequential manner (40%, 60%, 80% and 100%) for 10 min each and allowed to dry on a clean Petri dish at room temperature before observed by a SEM (JEOL ISM-5410) after gold coating.

For immunofluorescence staining of COL II, chondrocyte/cryogel constructs cultured for 21 d were fixed with 10% (w/v) formaldehyde overnight at 4 °C. After fixation, the constructs were washed three times in PBS containing 0.1% Tween 20 (PBST) for 30 min. Non-specific binding sites were blocked with the blocking buffer for 1 min and washed three times in PBST for 30 min. Mouse anti-COL II primary antibody (LSBio LS-C128248) was added and incubated overnight at 4 °C. The constructs were washed three times in PBST, and then incubated in anti-mouse IgG-Cy3 secondary antibody (Jackson ImmunoResearch Laboratories Inc. 115-165-003). After washing three times in PBST, the construct was incubated for additional 60 min at room temperature in 50 mg/ml DAPI for nuclear staining and washed three times in PBST for 30 min. The fluorescence-stained cells were visualized using a confocal laser scanning microscope (Leica TCS SP2).

2.5. Repair of full-thickness articular cartilage defect

The animal protocols were approved by the Institutional Animal Care and Use Committee of Chang Gung University and conformed to the standards of the Association for Assessment and Accreditation of Laboratory Animal Care. Before surgery, the rabbits were pre-anesthetized by the intramuscular injection of ketamine (20 mg/kg). Then the knee area of rabbit's hindlimb was shaved and prepared. General anesthesia was induced by applying 4% isoflurane, using a mask and maintained by the administration of 2% isoflurane with O_2 at 2.5 l/min. The rabbits were put in supine position and the surgical field was sterilized with iodine solutions; the non-sterile area was covered with sterile drapes. All surgical instruments were sterilized and kept sterile throughout the whole procedure. Through a 5.0-cm medial parapatellar incision approach, the knee joint was opened. Full-thickness defect (4 mm in diameter and 2 mm in thickness) was created through the articular cartilage and subchondral bone of the central patellar groove in 12 rabbits using an electric drill equipped with a 4-mm diameter drill bit. The animals were divided into three groups with four animals in each group. Group 1 was empty control, defects left un-treated. Group 2 was acellular cryogel, defect filled with a disk-shaped GCH-chitosan cryogel (4 mm in diameter and 2 mm in thickness). Group 3 was chondrocytes/cryogel, defect filled with a disk-shaped GCH-chitosan cryogel (4 mm in diameter and 2 mm in thickness) that was pre-seeded with 1×10^5 chondrocytes and cultured in DMEM/F12 for 14 d. After operation, the skins were closed with 4–0 Ethicon sutures, and 3 mg/kg gentamicin was administered intramuscularly as a prophylactic antibiotic. The wounds were sterilized and dressed with gentamicin ointments to prevent infection. All rabbits were allowed to move freely after surgery without plaster immobilization.

At 4 and 12 weeks, two animals from each group were euthanized with lethal doses of pentobarbital (0.5 g/kg bodyweight). The whole joint surfaces including the implants were dissected out for examination and photography. After gross evaluation, the samples were fixed in 10% formaldehyde, dehydrated in alcohol and embedded in paraffin, and sections were stained by hematoxylin and eosin (H&E), Alcian blue, Safranin O and immunohistochemical (IHC) staining of COL II. To determine the mechanical properties of the neocartilage at 12 weeks, the distal femur of 3 cm with entire joint surface was harvested from the experimental rabbits. The retrieved samples was polished at the bottom and placed in the ElectroForce 5200 BioDynamic Test Instrument. A custom-made probe (3 mm in diameter) was used to test the center of each repaired defect. The compression load was applied with a 250 N load cell at a cross-head speed of 0.005 mm/s from 0 to 0.5 mm displacement. A stress–strain curve was recorded with uniaxial stress.

2.6. Statistical analysis

All data are reported as mean ± standard deviation (SD). Statistics among multiple groups on cell proliferations and biochemical assays were carried out using one-way ANOVA test to determine significant differences. Tukey's post hoc test was used to determine the difference between any two groups with $p < 0.05$ considered statistically significant.

3. Results and discussion

3.1. Synthesis and characterization of cryogels

The percentage dry weight of each ECM component in hyaline cartilage is 15–20% COL II, 5–10% C6S, and 0.05–0.25% HA (weight

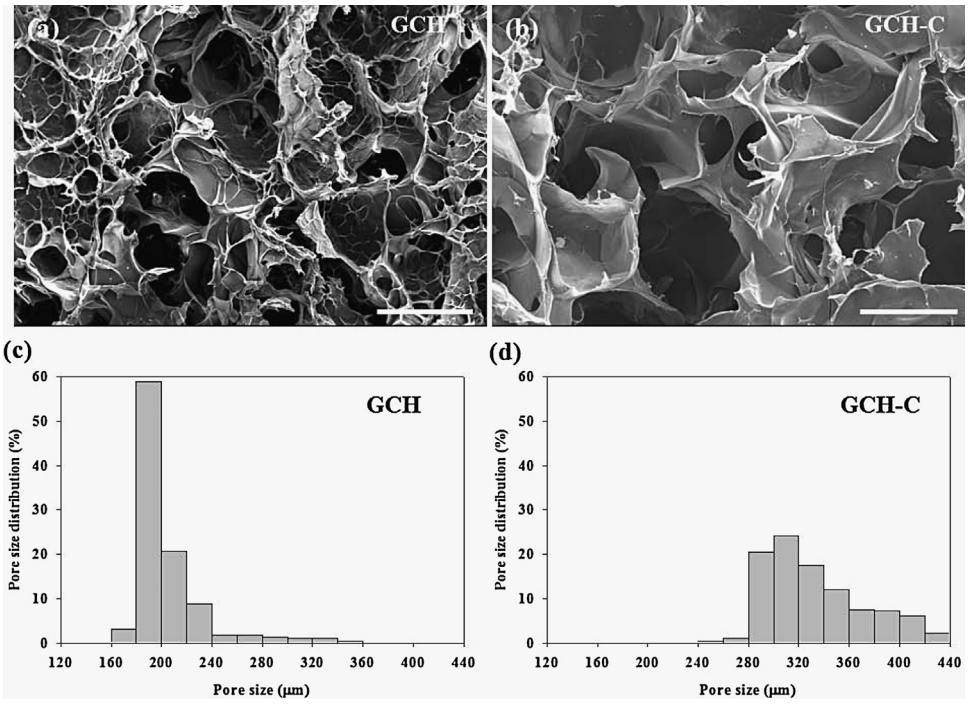

Fig. 1. Scanning electron micrograph (a, b) and pore size distribution (c, d) of cryogels. GCH, gelatin/chondroitin-6-sulfate/hyaluronan cryogel. GCH-C, gelatin/chondroitin-6-sulfate/hyaluronan/chitosan cryogel. Bar = 250 μm.

ratio = 3–4/1–2/0.01–0.5) (Maroudas, 1979). The GCH cryogel was thus prepared with a GEL/C6S/HA ratio of 4/1/0.05 to mimic the natural cartilage ECM component compositions with GEL replacing COL II. From SEM observation, both cryogels show open interconnected pore morphology. The pore diameter range is 100–350 μm for GCH and 100–500 μm for GCH-chitosan cryogel, with GCH-chitosan displaying thicker pore walls than GCH (Fig. 1a and b). A more accurate measurement of pore size and pore size distribution was provided by capillary flow porometry (Fig. 1c and d). The GCH cryogel shows sharp pore size distribution, with the minimum pore size being 160 μm and the maximum pore being 360 μm, and more than half of the pores are within 180–200 μm. The GCH-chitosan cryogel shows wider pore size distribution, with the minimum pore size being 240 μm and the maximum pore being 440 μm. The mean pore size increase from 199 to 286 μm after replacing 20% GEL with chitosan but does not show significant difference (Table 1). The GCH cryogel shows lower porosity than GCH-chitosan, which is similar to the trend observed for pore diameter.

An adequate porous structure of the scaffold is very important to allow cellular penetration into the construct. In addition, appropriate porous structures are required not to inhibit cellular growth and ECM secretion of the seeded chondrocytes after transplantation. In an earlier study, chitosan scaffolds with larger pores (70–120 μm) contained more chondrocytes, with more secreted COL II and GAGs than those with smaller pores (10–50 μm) after 28 d in vitro culture (Griffon, Sedighi, Schaeffer, Eurell, & Johnson, 2006). The authors proposed that larger interconnective pores improve the cellularity and ECM contents within the scaffold. Other experiments also showed that as the pores become larger, the rate of chondrocytes growth and GAG secretion increase. A pore size between 50 and 200 μm restricted GAGs secretion while a pore size between 250 and 500 μm provided better cell proliferation and ECM production (Lien, Ko, & Huang, 2009). That the pore size of GCH-chitosan cryogels is within in this range is expected to provide a better scaffold for cellular performance.

The compressive stress–strain behavior of cryogels was non-linear and can be fitted satisfactorily with the empirical non-linear model in equation (1) (Fig. 2a). The incorporation of chitosan in the cryogel increases the elastic modulus (or stiffness) and toughness (Table 2). GCH-chitosan shows higher compressive strain (2.5 folds) and can withstand 26 times more stress than GCH at failure. The strain energy to failure or the toughness of GCH-chitosan is also 63.8 times higher than that of GCH. GCH-chitosan shows elastic behavior till around 60% compression; in contrast, GCH exhibits a more pronounced increase in modulus leading up to failure. Thus, the elastic moduli (slopes of stress–strain curves) of GCH-chitosan are 5 and 1.3 times that of GCH at 10% and 30% deformation, respectively. The Young's modulus of human knee articular cartilages was from 0.58 to 0.85 MPa (Jurvelin, Buschmann, & Hunziker, 2003). Therefore, GCH-chitosan is evidently more appropriate

Table 1
Pore size and porosity of cryogels. Values are the mean ± SD of five independent measurements.

	GCH	GCH-chitosan
Average pore size (μm)	199 ± 14	286 ± 95
Porosity (%)	74.7 ± 2.7	97.1 ± 2.0*

* $p < 0.05$ compared with GCH.

Table 2
Mechanical properties of cryogels. Values are the mean ± SD of five independent measurements.

	GCH	GCH-chitosan
Compressive elastic modulus at $\varepsilon = 0.1$ (kPa)	49.9 ± 0.7	254.1 ± 45.1*
Compressive elastic modulus at $\varepsilon = 0.3$ (kPa)	503.6 ± 88.4	638.6 ± 95.3*
Compressive strain to failure, ε_{max} (%)	38.7 ± 1.3	96.8 ± 0.9*
Compressive stress to failure, σ_{max} (kPa)	111.1 ± 4.6	2869.3 ± 243.3*
Compressive strain energy to failure (kJ/m^3)	10.1 ± 0.4	644.6 ± 57.9*
Compression energy (kJ/m^3)	4.4 ± 0.2	7.7 ± 0.3*
Relaxation energy (kJ/m^3)	1.2 ± 0.1	2.5 ± 0.2*
Dissipation energy (kJ/m^3)	2.7 ± 0.1	5.2 ± 0.2*
Percentage of energy dissipation (%)	61.6 ± 1.2	67.1 ± 2.0*

* $p < 0.05$ compared with GCH.

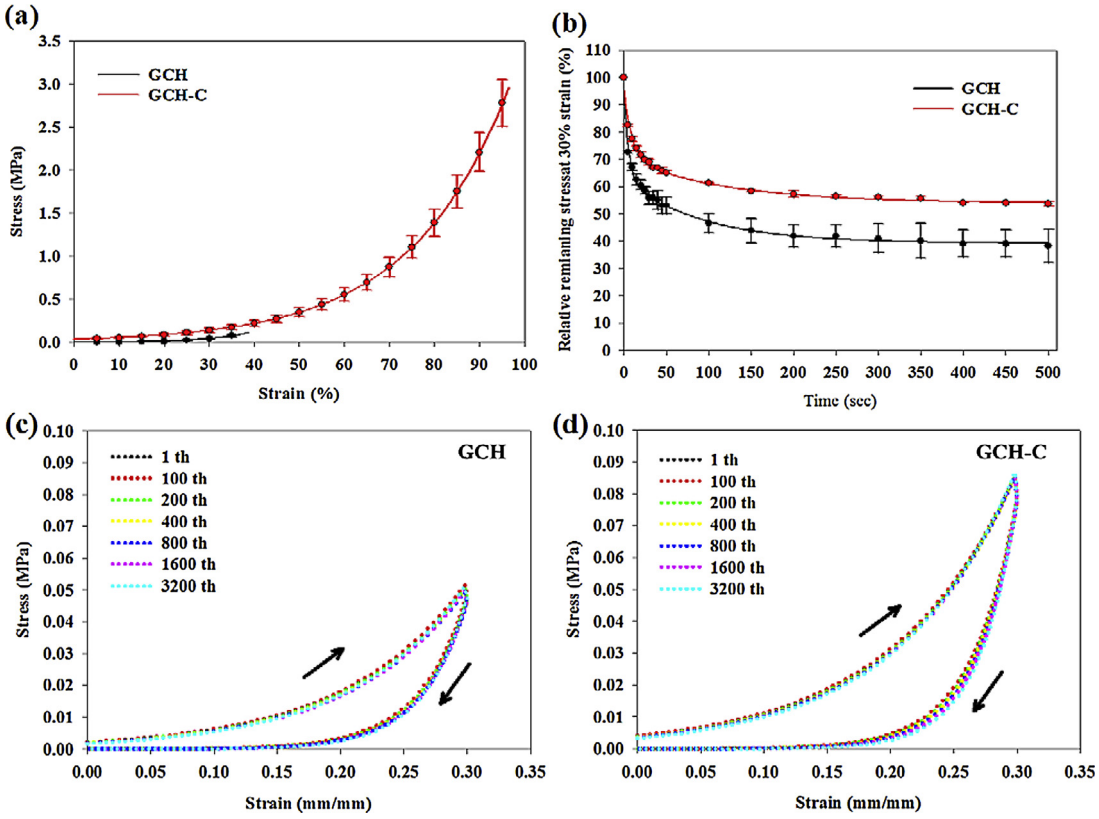

Fig. 2. Compressive mechanical properties of cryogels. (a) The stress–strain curve. (b) The stress relaxation at strain of 0.3. (c, d)The loading–unloading hysteresis curves during 3200 successive compressions to a maximum strain of 0.3. GCH, gelatin/chondroitin-6-sulfate/hyaluronan cryogel. GCH-C, gelatin/chondroitin-6-sulfate/hyaluronan/chitosan cryogel.

for cartilage tissue engineering than GCH judging from its elastic modulus is within this range.

Compressive stress relaxation assesses the mechanical stability of cryogels. This is especially important for ensuring that cryogels will not deform to an unacceptable level during prolonged static loading. Fig. 2b shows a typical set of the stress relaxation data accompanied by Eq. (2) curve fitting. The initial stress relaxation rate (k_1) is significantly lower for GCH-chitosan (0.11) than GCH (0.20), however, the final stress relaxation rate (k_2) for all formulations are similar (0.011). GCH needs shorter time to completely release stress, thus alleviates the extent of damage to the scaffold than GCH-chitosan. However, the relative remaining stress of GCH-chitosan is 54%, which is significant higher than that of GCH (39%), indicating GCH-chitosan cryogel has higher support force and provides more stable mechanical responses when stressed.

From the results of cyclic compression testing, a hysteresis loop exists in the stress–strain curve (Fig. 2c and d). The GCH-chitosan cryogel dissipates more energy during compression, both on an absolute value and a percent dissipation basis than GCH, thus is expected to perform better than GCH in terms of energy dissipation (Table 2). The percentage energy dissipation of all cryogels is similar to that of cartilage reported in the literature, which is from 50% to 80% (Varga et al., 2007). Overall, the mechanical properties of GCH-chitosan were significantly better than those of GCH. This can be ascribed to the fact that chitosan was present in the GCH-chitosan strut, resulting in higher resistance to mechanical compression. The superior recovery property of cryogel from large strains could be shown from the same hysteresis curves during successive loading–unloading cycles at 30% maximum strain, which result in a constant dissipation energy during each cycle. This unique feature contributes to the development of cryogel as a tough scaffold for cartilage tissue engineering, which can recover from large strains and absorb impacts without permanent damage.

The viscoelastic behavior of cryogels with the storage (E') and viscous (E'') modulus measured from 0.5 to 10 Hz is shown in Fig. 3a. The loss modulus is very small and comparable. The GCH-chitosan cryogel has a storage modulus higher than GCH cryogel (2.22 vs. 1.56 MPa), which represents the elastic component of a material. The constitutive properties of porcine cartilage tissue have been measured in the range 1–20 Hz. The storage modulus is almost insensitive to frequency, and has a value of 9 MPa at frequency between 10 and 20 Hz. However, at lower frequency below 10 Hz, the storage modulus of porcine cartilage tissue changes sharply to about 3 MPa (Franke, Göken, Meyers, Durst, & Hodge, 2011). The GCH-chitosan cryogel has a higher storage modulus than GCH cryogel and is more closely match these values of native cartilage at high strains. The loss tangent (tan δ) shown in Fig. 3b provides information about the viscoelastic properties, the smaller the loss tangent is, the more elastic is the material. The value of tan δ is lower for GCH-chitosan, indicating chitosan incorporation enhances cryogel elasticity. The phase angle (δ) of human articular cartilage tissue was reported to be about 14° (Ronken et al., 2012). Such a small phase angle indicates a small viscous response in cartilage tissue at the frequencies reported. In this study, both cryogels show a very small phase angle and highly elastic nature, which is similar to that reported for cartilage but at a low value ($\delta \equiv 6°$).

3.2. *In vitro* cell culture

As a natural polysaccharide that is structurally similar to GAGs, chitosan shares some characteristics with various GAGs and HA present in articular cartilage (Muzzarelli, 2009). Incorporation of chitosan in GCH cryogel for improvement into a four-component

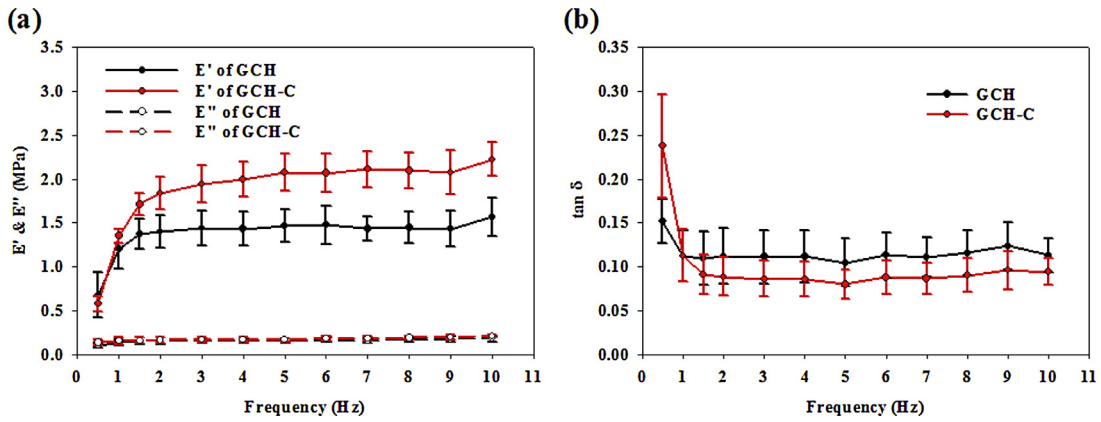

Fig. 3. The viscoelastic properties of cryogels determined by dynamic compression testing. (a) Storage modulus (E') and loss modulus (E''). (b) Loss tangent (tan δ). Strain = 30%. GCH, gelatin/chondroitin-6-sulfate/hyaluronan cryogel. GCH-C, gelatin/chondroitin-6-sulfate/hyaluronan/chitosan cryogel.

composite cartilage tissue engineering scaffold appears to be a logical approach for enhancing chondrogenesis (Di Martino, Sittinger, & Risbud, 2005). Both cryogel scaffolds supported cell attachment and growth, and chondrogenic phenotype. A significant difference in cell number was found from day 7 to 21 with more cells found in GCH (Fig. 4a). The reduced growth rate for GCH-chitosan corresponds to previous studies suggesting chitosan partially inhibits the cell cycle in G1 phase (Mao et al., 2004). The value of normalized sGAG production (sGAG/DNA) is shown in Fig. 4b. The sGAG production increases with time and plateaus at day 14 in GCH while it could be maintains up to 21 d in GCH-chitosan. Also, a reverse trend from cell proliferation, the sGAG production is significantly higher in GCH-chitosan after day 7. The values of normalized COL II production (COL II/DNA) in both cryogels increase continuously from day 5 to day 14. Nonetheless, the specific secretion of COL II is significant higher in GCH-chitosan from 7 to 21 d and GCH-chitosan could maintain the COL II production to the end of culture period in contrast to a decline trend after 14 d for GCH (Fig. 4**c**).

Seeded chondrocytes show vast enhancement of COL II production and to a less extent sGAG production in both cryogels compared with chondrocytes before seeding (Fig. 4b and c). Compared with chondrocytes before seeding, the sGAG value in GCH is higher only at day 14, but the value is significant higher in GCH-chitosan from 7 to 21 d. At day 14, the enhancement of COL II production is 21.8 times and 18.2 times for GCH-chitosan and GCH, respectively. The chondrocyte are known to easily lose their differentiated phenotype in two-dimensional culture (Schnabel et al., 2002). The dedifferentiation process is accompanied by a shift toward a fibroblast-like phenotype and loss of COL II production ability (Malda et al., 2003). However, this process is reversible because dedifferentiated chondrocytes can recover their differentiated phenotype when they are relocated into a three-dimensional environment (Hoemann, Sun, Legare, McKee, & Buschmann, 2005). Seeding chondrocytes from two-dimensional culture to three-dimensional environment like cryogels apparently induces the cells to re-acquire a chondrocyte-specific phenotype and produce a cartilaginous-like tissue in vitro (Vinatier, Mrugala, Jorgensen, Guicheux, & Noel, 2009).

The morphology of chondrocytes and the deposition of ECM in cryogel were further analyzed by SEM and confocal microscopy. Globular, chondrocyte-like cells are well adhered to the wall of GCH-chitosan cryogel scaffold and surrounded by a thick ECM layer (Fig. 5a). Cells within GCH cryogel show a more flat cell shape but still show abundant ECM secretion. Specifically, the cartilage-specific ECM molecule COL II could be identified from immunofluorescence staining and lining along the cryogel wall, where chondrocytes could be identified from nuclear staining (Fig. 5b). The GCH-chitosan cryogel is seen to better preserve the spherical chondrocytic morphology and the expression of COL II, a marker of differentiated chondrocytes. This could be contributed from the effect of incorporating chitosan or the biomechanical property of GCH-chitosan, which is more comparable to that of cartilage tissue than GCH. Overall, this trend is consistent with silk fibroin/chitosan or collagen/chitosan/chondroitin sulfate spongy scaffolds, where incorporation of chitosan could provide a scaffold with more favorite chondrogenic properties (Lee et al., 2005; Bhardwaj et al., 2011). The GCH-chitosan cryogel was thus chosen for in vivo studies.

3.3. *Repair of full-thickness articular cartilage defect*

From gross observation, there was no animal death, infection, wound dehiscence or disability during 3 months of observation (Fig. 6a). One month after implantation, the defects were mostly

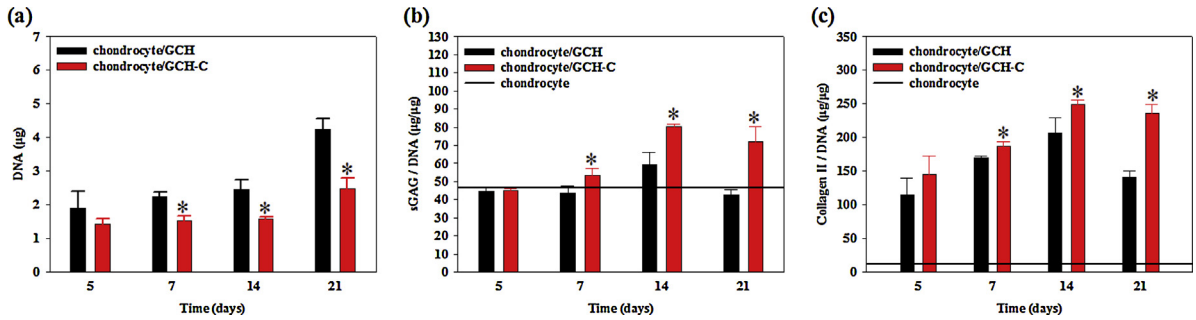

Fig. 4. Proliferation and extracellular matrix production of chondrocytes before seeding and chondrocytes cultured in cryogels at different time points. (a) DNA content, (b) sulfated glycosaminoglycan (sGAG) content normalized to DNA content, (c) collagen type II content normalized to DNA content. GCH, gelatin/chondroitin-6-sulfate/hyaluronan cryogel. GCH-C, gelatin/chondroitin-6-sulfate/hyaluronan/chitosan cryogel. $^*p < 0.05$ compared with GCH.

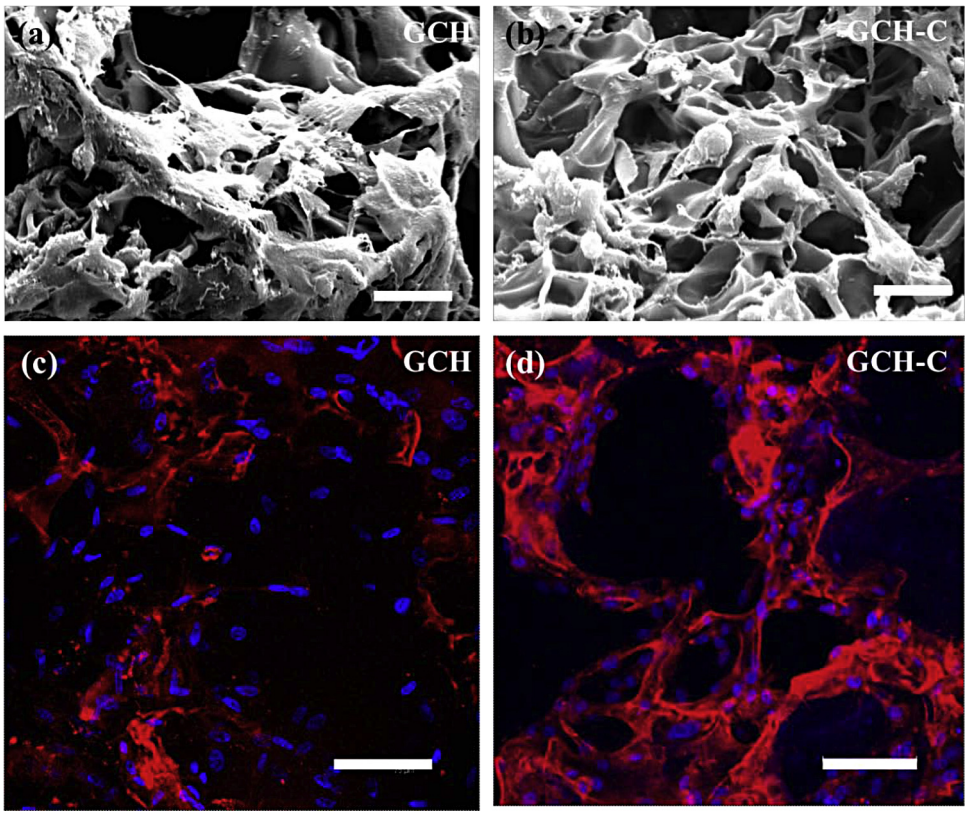

Fig. 5. (a, b) Scanning electron microscope (bar = 20 μm), (c, d) confocal laser scanning microscope micrographs of chondrocytes cultured for 21 d in cryogels (bar = 75 μm). Collagen type II was stained red by immunostaining and cell nuclei stained blue by DAPI. GCH, gelatin/chondroitin-6-sulfate/hyaluronan cryogel. GCH-C, gelatin/chondroitin-6-sulfate/hyaluronan/chitosan cryogel.

filled with fibrous tissue with a concavity toward the center in the empty control group. In the acellular cryogel group, the defects had not been fully filled with the repair tissue with sharply defined margins and clearly visible edges. In the chondrocytes/cryogel group, the defects were filled with smooth, white and semi-transparent tissue but the boundary of the defects could be recognized and the density of neocartilage was slightly different from the surrounding native cartilage. After 3 months, there were still a large vacant in the center and only a thin layer of white and rough fibrous tissue in the defect in the empty control group. In the acellular cryogel group, the defect was almost filled with cartilage-like tissues of similar color to the surrounding cartilage. However, there was a discernable circular junction between the new and normal tissue. Slight central depression with rough surface of repaired tissue was also noted. The defect in the chondrocytes/cryogel group was completely covered with semitransparent tissue which was similar to the adjacent normal cartilage. It was difficult to recognize the native cartilage from the repaired tissue and the defect margins were almost disappeared.

From histological examination, the H&E stain shows only marginal cartilage formation with much fibrous tissue at the defects in the empty control group after 1 or 3 month (Fig. 6b). This implies that the size of defect is not able to recover without additional assistance. The Safranin O stain yields the proteoglycan that is rich in newly formed tissues and lacuna (Fig. 6c). Alcian blue stain highlights the sGAG that is constituted by chondroitin sulfate secreted by newly formed chondrocytes (Fig. 6d). In the acellular cryogel group, a thin layer of neocartilage over the residual cryogel was observed after 1 month. Scanty of chondrocytes ingrowth within the scaffold was also noticed. After 3 months, restoration of cartilage and subchondral bone is seen in Safranin O and Alcian blue stains although the density of lacuna and thickness are lesser and thinner compared with the surrounding native cartilage. The integration between neocartilage and adjacent native cartilage was incomplete and the surface of defects was slightly concave. In the chondrocytes/cryogel group, chondrocytes are arranges in two orders: parallel to joint surface at the top of the cryogel and scattered randomly within the residual cryogel after 1 month. The scattered cartilage tissues are likely to be originating from seeded chondrocytes, and the stain was lighter in the newly formed tissues from Safranin O and Alcian blue stains. The integration between neocartilage and adjacent native cartilage is incomplete. After 3 months, the scaffolds are totally degraded and chondrocytes are much more orderly in their arrangement from bottom to top. The neocartilage is much thicker compared with the acellular cryogel group although it is still slightly thinner than the normal articular cartilage. The surface is smooth and the integration between the newly formed cartilage and the surrounding native cartilage is complete. Subchondral bone at defect is restored with no obvious gap between the newly formed hyaline-like cartilage.

To further evaluate the composition of these newly formed tissues, COL II was evaluated by IHC staining (Fig. 6e). The secretion of COL II is relatively low in the first month in either acellular or chondrocytes/cryogel group. At the third month, the overall expression is much higher in chondrocytes/cryogel group than in acellular cryogel group, indicating the better differentiation and proliferation of chondrocytes in GCH-C cryogel in vivo for neocartilage formation (Vinatier, Mrugala, Jorgensen, Guicheux, & Noel, 2009).

Since the knee joint cartilage is important for weight-bearing of body, it is crucial to evaluate the mechanical property of tissue engineered cartilage. After 3 months, the entire knee joint including implants and surrounding tissues were carefully harvested for mechanical testings and the elastic modulus at $\varepsilon = 0.1$ was calculated from the stress–strain curve (Fig. 6f). The elastic modulus

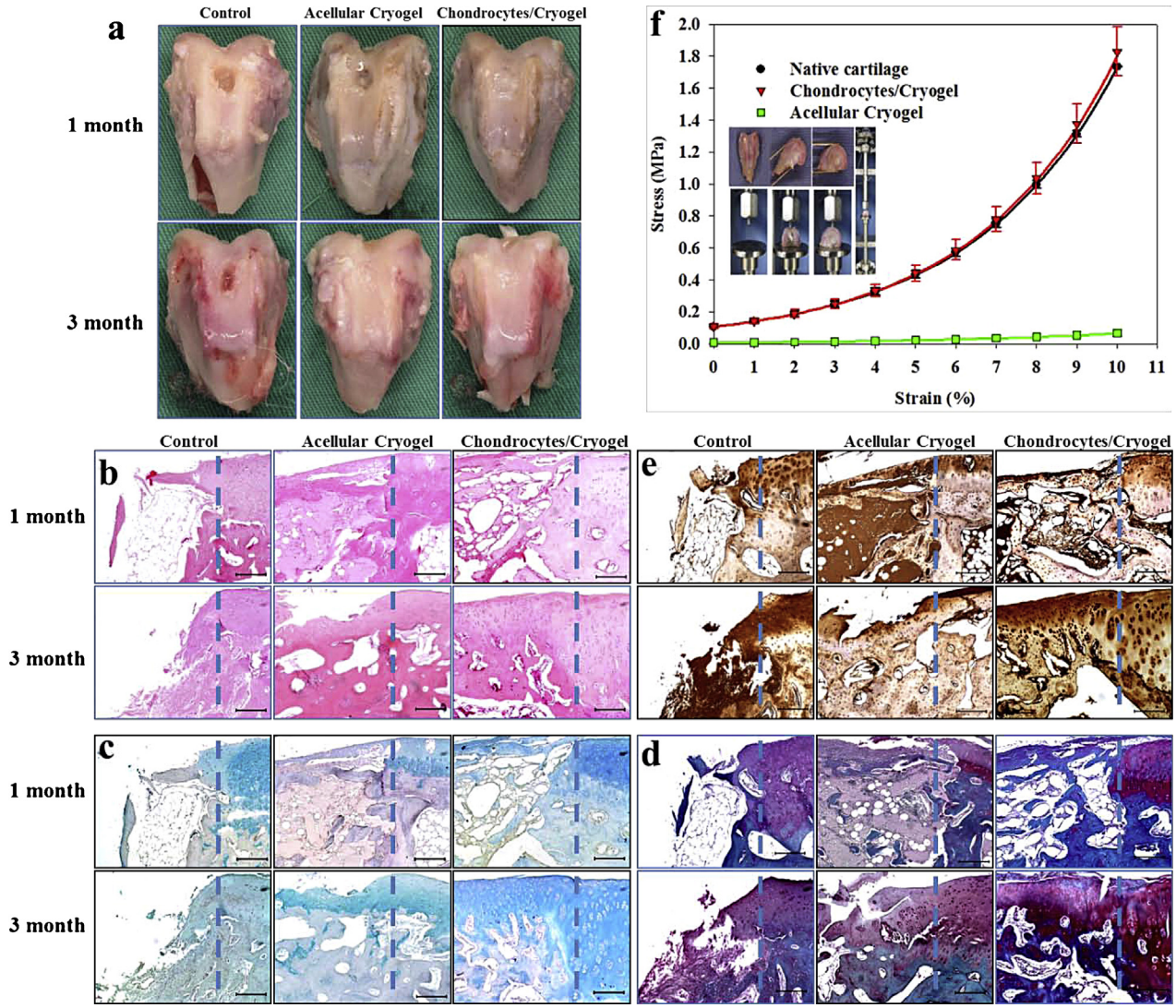

Fig. 6. Gross observation (a), hematoxylin and eosin (H&E) (b), Alcian blue (c), Safranin O (d) and collagen type II immunohistochemical (e) stainings of the explanted samples 1 and 3 months post-implantation. The rabbit cartilage defect was not treated (control), filled with gelatin/chondroitin-6-sulfate/hyaluronan/chitosan cryogel (acellular cryogel), or chondrocytes-seeded gelatin/chondroitin-6-sulfate/hyaluronan/chitosan cryogel (chondrocytes/cryogel). The defect creation boundary is shown as the dotted line in each panel with native cartilage to the right. Bar = 200 μm. (f) Comparison of the stress–strain curves of native cartilage, acellular cryogel and chondrocytes/cryogel 3 months post-implantation. The lines are best-fit curves from Eq. (1). The insert illustrates the setup for mechanical testing.

of acellular cryogel after implantation is 1.46 ± 0.37 MPa, which is 5.84 folds that of cryogel before implantation (Table 2). The elastic modulus of the neocartilage in the chondrocytes/cryogel group is 35.5 folds that of the acellular cryogel group at 51.9 ± 3.3 MPa. Most importantly, there is no significant difference in the elastic modulus between the chondrocytes/cryogel group and the native cartilage (48.1 ± 1.8 MPa), indicating the regenerated cartilage is mechanically functional to repair cartilage defect.

4. Conclusions

We have demonstrated that macroporous elastic cryogels could be fabricated from cartilage ECM components with similar compositions. The cryogel is endowed with high porosity, large pore size, and unique mechanical properties such as high elasticity, moderate toughness and total recovery from large strains. GCH-chitosan cryogel synthesized by replacing 20% GEL with chitosan provides a scaffold with improved physical and mechanical properties. The comparable biomechanical properties to those of cartilage make GCH-chitosan cryogel a suitable scaffold for cartilage tissue engineering. Growth arrest and enhanced sGAG and COL II secretion of chondrocyte suggests redifferentiation of chondrocytes in GCH-chitosan cryogel. Based on Alcian blue, Safranin O and IHC stains of the chondrocytes phenotypic markers (sGAG, proteoglycan and COL II) and the elastic modulus of the neocartilage, successful cartilage tissue engineering using allogeneic chondrocytes in GCH-chitosan cryogel could be demonstrated for functional repair of full-thickness articular cartilage defects in rabbits.

Acknowledgements

Financial supports from the National Science Council and Chang Gung Memorial Hospital (CRRPD5C0201 and CMRPD3D0201) are appreciated. The technical assistance from the Microscopy Core Laboratory, Chang Gung Memorial Hospital is also acknowledged.

References

Angele, P., Muller, R., Schumann, D., Englert, C., Zellner, J., Johnstone, B., et al. (2009). Characterization of esterified hyaluronan-gelatin polymer composites suitable for chondrogenic differentiation of mesenchymal stem cells. *Journal of Biomedical Materials Research A, 91*, 416–427.

Bhardwaj, N., Nguyen, Q. T., Chen, A. C., Kaplan, D. L., Sah, R. L., & Kundu, S. C. (2011). Potential of 3-D tissue constructs engineered from bovine chondrocytes/silk fibroin-chitosan for in vitro cartilage tissue engineering. *Biomaterials*, *32*, 5773–5781.

Chang, C. H., Liu, H. C., Lin, C. C., Chou, C. H., & Lin, F. H. (2003). Gelatin–chondroitin–hyaluronan tri-copolymer scaffold for cartilage tissue engineering. *Biomaterials*, *24*, 4853–4858.

Chang, K. H., Liao, H. T., & Chen, J. P. (2013). Preparation and characterization of gelatin/hyaluronic acid cryogels for adipose tissue engineering: In vitro and in vivo studies. *Acta Biomaterialia*, *9*, 9012–9026.

Chen, J. P., & Cheng, T. H. (2006). Thermo-responsive chitosan-graft-poly(N-isopropylacrylamide) injectable hydrogel for cultivation of chondrocytes and meniscus cells. *Macromolecular Bioscience*, *6*, 1026–1039.

Di Martino, A., Sittinger, M., & Risbud, M. V. (2005). Chitosan: A versatile biopolymer for orthopaedic tissue-engineering. *Biomaterials*, *26*, 5983–5990.

Enobakhare, B. O., Bader, D. L., & Lee, D. A. (1996). Quantification of sulfated glycosaminoglycans in chondrocyte/alginate cultures, by use of 1,9-dimethylmethylene blue. *Analical Biochemistry*, *243*, 189–191.

Franke, O., Göken, M., Meyers, M. A., Durst, K., & Hodge, A. M. (2011). Dynamic nanoindentation of articular porcine cartilage. *Materials Science and Engineering: C*, *31*, 789–795.

Griffon, D. J., Sedighi, M. R., Schaeffer, D. V., Eurell, J. A., & Johnson, A. L. (2006). Chitosan scaffolds: Interconnective pore size and cartilage engineering. *Acta Biomaterialia*, *2*, 313–320.

Hoemann, C. D., Sun, J., Legare, A., McKee, M. D., & Buschmann, M. D. (2005). Tissue engineering of cartilage using an injectable and adhesive chitosan-based cell-delivery vehicle. *Osteoarthritis and Cartilage*, *13*, 318–329.

Jurvelin, J. S., Buschmann, M. D., & Hunziker, E. B. (2003). Mechanical anisotropy of the human knee articular cartilage in compression. *Proceedings of the Institute of Mechanical Engineers, Part H: Journal of Engineering in Medicine*, *217*, 215–219.

Kim, Y. J., Sah, R. L., Doong, J. Y., & Grodzinsky, A. J. (1988). Fluorometric assay of DNA in cartilage explants using Hoechst 33258. *Analytical Biochemistry*, *174*, 168–176.

Lee, J. E., Jeong, M. H., Ahn, H. J., Kim, J. K., Choi, K., & Chang, C. B. (2005). Evaluation of chondrogenesis in collagen/chitosan/glycosaminoglycan scaffolds for cartilage tissue engineering. *Journal of Tissue Engineering and Regenerative Medicine*, *2*, 41–49.

Lien, S.-M., Li, W.-T., & Huang, T.-J. (2008). Genipin-crosslinked gelatin scaffolds for articular cartilage tissue engineering with a novel crosslinking method. *Materials Science and Engineering: C*, *28*, 36–43.

Lien, S. M., Ko, L. Y., & Huang, T. J. (2009). Effect of pore size on ECM secretion and cell growth in gelatin scaffold for articular cartilage tissue engineering. *Acta Biomaterialia*, *5*, 670–679.

Lozinsky, V., Plieva, F., Galaev, I., & Mattiasson, B. (2001). The potential of polymeric cryogels in bioseparation. *Bioseparation*, *10*, 163–188.

Lozinsky, V. I., Galaev, I. Y., Plieva, F. M., Savina, I. N., Jungvid, H., & Mattiasson, B. (2003). Polymeric cryogels as promising materials of biotechnological interest. *Trends in Biotechnology*, *21*, 445–451.

Malda, J., van Blitterswijk, C. A., Grojec, M., Martens, D. E., Tramper, J., & Riesle, J. (2003). Expansion of bovine chondrocytes on microcarriers enhances redifferentiation. *Tissue Engineering*, *9*, 939–948.

Mao, J. S., Cui, Y. L., Wang, X. H., Sun, Y., Zhao, H. M., & Yao, K. D. (2004). A preliminary study on chitosan and gelatin polyelectrolyte complex cytocompatibility by cell cycle and apoptosis analysis. *Biomaterials*, *25*, 3973–3981.

Maroudas, A. (1979). Physicochemical properties of articular cartilage. In *Adult Articular Cartilage* (2nd ed., pp. 189–290). Freeman MAR London: Pitman Medical.

Muzzarelli, R. A. A. (2009). Chitins and chitosans for the repair of wounded skin, nerve, cartilage and bone. *Carbohdrate Polymers*, *76*, 167–182.

Muzzarelli, R. A. A., Greco, F., Busilacchi, A., Sollazzo, V., & Gigante, A. (2012). Chitosan, hyaluronan and chondroitin sulfate in tissue engineering for cartilage regeneration: A review. *Carbohydrate Polymers*, *89*, 723–739.

Nettles, D. L., Elder, S. H., & Gilbert, J. A. (2002). Potential use of chitosan as a cell scaffold material for cartilage tissue engineering. *Tissue Engineering*, *8*, 1009–1016.

Ronken, S., Arnold, M. P., Ardura Garcia, H., Jeger, A., Daniels, A. U., & Wirz, D. (2012). A comparison of healthy human and swine articular cartilage dynamic indentation mechanics. *Biomechanics and Modeling in Mechanobiology*, *11*, 631–639.

Schnabel, M., Marlovits, S., Eckhoff, G., Fichtel, I., Gotzen, L., Vecsei, V., et al. (2002). Dedifferentiation-associated changes in morphology and gene expression in primary human articular chondrocytes in cell culture. *Osteoarthritis and Cartilage*, *10*, 62–70.

Sechriest, V. F., Miao, Y. J., Niyibizi, C., Westerhausen-Larson, A., Matthew, H. W., Evans, C. H., et al. (2000). GAG-augmented polysaccharide hydrogel: A novel biocompatible and biodegradable material to support chondrogenesis. *Journal of Biomedical Materials Research*, *49*, 534–541.

Solchaga, L. A., Goldberg, V. M., & Caplan, A. I. (2001). Cartilage regeneration using principles of tissue engineering. *Clinical Orthopaedics and Related Research*, *391*, S161–S170.

Swieszkowski, W., Ku, D. N., Bersee, H. E., & Kurzydlowski, K. J. (2006). An elastic material for cartilage replacement in an arthritic shoulder joint. *Biomaterials*, *27*, 1534–1541.

Vacanti, J. (2003). Tissue and organ engineering: Can we build intestine and vital organs? *Journal of Gastrointestinal Surgery*, *7*, 831–835.

VandeVord, P. J., Matthew, H. W., DeSilva, S. P., Mayton, L., Wu, B., & Wooley, P. H. (2002). Evaluation of the biocompatibility of a chitosan scaffold in mice. *Journal of Biomedical Materials Research*, *59*, 585–590.

Varga, F., Drzik, M., Handl, M., Chlpik, J., Kos, P., Filova, E., et al. (2007). Biomechanical characterization of cartilages by a novel approach of blunt impact testing. *Physiological Research*, *56*, S61–S68.

Vinatier, C., Mrugala, D., Jorgensen, C., Guicheux, J., & Noel, D. (2009). Cartilage engineering: A crucial combination of cells, biomaterials and biofactors. *Trends in Biotechnology*, *27*, 307–314.

Wan, W. K., Campbell, G., Zhang, Z. F., Hui, A. J., & Boughner, D. R. (2002). Optimizing the tensile properties of polyvinyl alcohol hydrogel for the construction of a bioprosthetic heart valve stent. *Journal of Biomedical Materials Research*, *63*, 854–861.

Woo, S. L., Gomez, M. A., & Akeson, W. H. (1981). The time and history-dependent viscoelastic properties of the canine medical collateral ligament. *Journal of Biomechanical Engineering*, *103*, 293–298.

Yang, J., Webb, A. R., Pickerill, S. J., Hageman, G., & Ameer, G. A. (2006). Synthesis and evaluation of poly(diol citrate) biodegradable elastomers. *Biomaterials*, *27*, 1889–1898.

Zhang, R., & Ma, P. X. (1999). Poly(α-hydroxyl acids)/hydroxyapatite porous composites for bone-tissue engineering. I. Preparation and morphology. *Journal of Biomedical Materials Research*, *44*, 446–455.